Supplementary Information

Eutectogel-based biomimetic barrier with network-structure-transformation-activated defensive and reparative functions for infected wounds

Hui Sun,[a] Jing Cheng,[a] Xu Peng,[b] Mengyan Kang,[c] Ao Gao,[c] Jun Luo,[a] Xinyuan Xu*[a] and Jianshu Li*[ad]

[a] College of Polymer Science and Engineering, State Key Laboratory of Advanced Polymer Materials, Sichuan University, Chengdu, 610065, P.R. China

[b] Experimental and Research Animal Institute, Sichuan university, Chengdu, 610041, P.R. China

[c] School of Life Science and Engineering, Southwest Jiaotong University, Chengdu, 610031, P.R. China

[d] State Key Laboratory of Oral Diseases, Med-X Center for Materials, West China Hospital of Stomatology, Sichuan University, Chengdu, 610041, P.R. China

E-mail: xinyuanxu22@scu.edu.cn, jianshu_li@scu.edu.cn

1 Experimental section

1.1 Materials

[2-(Methacryloyloxy)ethyl]dimethyl-(3-sulfopropyl)ammonium hydroxide (SBMA) was purchased from TCI (China). Carvacrol (CA) was purchased from Sigma-Aldrich (USA). 2-Hydroxy-2-methylpropiophenone (I1173), ethylene dimethacrylate (EDMA), 1,1-diphenyl-2-picrylhydrazyl (DPPH) and terephthalic acid (PTA) were purchased from Aladdin (China). Hydrogen peroxide (H_2O_2) and ferrous sulfate were purchased from Kelong Chemicals (China). Nutrient agar, Luria-Bertani (LB) broth powder, calcein-AM, propidium iodide (PI), TRITC-phalloidin, dihydrochloride (DAPI), 2',7'-dichlorodihydrofluorescein diacetate (DCFH-DA) and lipopolysaccharides (LPS) were purchased from Solaribo (China). 2,2'-Azinobis (3-thylbenzothiazoline-6-sulfonic acid ammonium salt) (ABTS) free radicals scavenging kit, BCA protein assay kit and live bacteria staining kit (N, N-dimethylaniline N-oxide, DMAO) were purchased from Beyotime (China). Fetal bovine serum (FBS), phosphate buffered saline (PBS), trypsin and Dulbecco's modified eagle medium (DMEM) were purchased from Gibico (USA). Penicillin-streptomycin solution was obtained from Hyclone (USA). Cell-counting Kit (CCK-8) was purchased from APExBIO (USA). PE anti-mouse CD86 antibody and APC anti-mouse CD206 antibody were purchased from Elabscience (China). Tissue fixative, tissue RNA preservation solution and chemicals for histological staining were purchased from Servicebio (China). Ultrapure water (UP water) obtained on a Milli-Q water purification system (Essential 5, Millipore) was used throughout.

1.2 Synthesis and characterization of SBMA/CA (SC) DES

SBMA and CA with different molar ratios were mixed and stirred at 60°C until the mixture was clear and transparent. Differential scanning calorimetry (DSC) analysis was performed on a DSC instrument (DSC3+, Mettler) over the temperature range of -70 to 30°C at a heating rate of 5 °C/min under a nitrogen atmosphere. Thermogravimetry analysis (TGA) was performed on TG analyser (TGA2, Mettler) over the temperature range of 30 to 600°C at a heating rate of 10 °C/min under a nitrogen atmosphere. Fourier transform infrared (FT-IR) spectra of SBMA, CA and SC DES were obtained on a FT-IR spectrometer (Nicolet iS50, Thermo Fisher).

1.3 Fabrication and characterization of PSC eutectogels

Certain amount of crosslinker (EDMA) and photoinitiator (I1173, 2 mol% to total double bonds) were added into freshly prepared SC DES and the mixture was stirred for 10 min to obtain a homogeneous liquid.

Then the mixture was centrifuged to remove bubbles, transferred into a teflon mold and exposed to an ultraviolet light (365 nm, 200W) for 5 min to obtain polymerized SBMA/CA DES (denoted as PSC eutectogel). The PSC eutectogels were named after "PSC-x" in which x represented the molar percentage of EDMA to total double bonds. The composition of PSC-x eutectogels was listed in Table S4, Supplementary Information.

The IR spectra of the release medium was recorded using an in-situ IR detector (ReactIR 702L, Mettler). CA release behaviour from PSC eutectogels was measured using an ultraviolet-visible (UV-vis) spectrophotometer (TU1901, Persee). The content of PSC-x eutectogels was fixed to 1 mg/mL in PBS, and then these samples were placed in a 37 °C constant temperature shaking bath. The released CA amount was calculated by measuring the absorbance of supernatant at 273 nm based on a standard curve of CA. The storage modulus and loss modulus of PSC eutectogels (8 mm in diameter and 2 mm in thickness) were measured on a rotational rheometer (MCR302, Anton Paar) at strain sweep (0.01-1%, 25 Hz) and frequency sweep (0.1-10 rad/s, 0.1%) mode. The critical relaxation exponent was obtained by power correlation function fitting of the G' from frequency sweep. Low-field solid-state NMR spectroscopy of the PSC eutectogels was conducted using an NMR analyser (VTMR-20-010V, Niumag) with parameter setting same to reported literature.[1]

1.4 In vitro radicals scavenging properties of PSC eutectogels

The Fenton reaction between H_2O_2 and Fe^{2+} was utilized to test the scavenging effect of PSC-x eutectogels on hydroxyl radicals. 15 mg of the eutectogel was incubated with 1 mL PBS, 700 μL PTA solution (3 mg/mL), 700 μL H_2O_2 solution (0.1 nM) and 700 μL $FeSO_4$ solution (2.5 mg/mL) at 25 °C for 2 h in the dark. For control and blank group, the sample and H_2O_2 solution were replaced by 15 and 700 μL UP water respectively without other operations. After incubation, the fluorescence intensity from 350 nm to 550 nm of the supernatant was measured on a fluorescence spectrophotometer (RF-6000, Shimadzu). The excitation wavelength was at 315 nm. The scavenging ratio of hydroxyl radicals was calculated by the following equation:

$$Scavenging\ ratio\ of\ \cdot OH\ (\%) = \frac{FL_{sample} - FL_{blank}}{FL_{control} - FL_{blank}} \times 100\%$$

Where FL_{sample}, FL_{blank} and $FL_{control}$ represented the fluorescence intensity of the sample, blank and control group respectively.

Then, the scavenging activity of PSC-x eutectogels on DPPH was evaluated according to reported protocol. 10 mg of the sample was incubated with 2 mL DPPH solution (0.2 mg/mL in 80% ethanol) at 37 °C for 30 min. The absorbance of the supernatant at 517 nm was recorded on a microplate reader (SpectraMax ABS plus, Molecular Devices). The sample was replaced by 10 μL UP water to set as the control group. The scavenging ability of PSC-x eutectogels on DPPH radicals was obtained by the following equation:

$$Scavenging\ ratio\ of DPPH\ (\%) = (1 - \frac{A_{sample}}{A_{control}}) \times 100\%$$

Where A_{sample} and $A_{control}$ represented the absorbances of the sample and control group respectively.

The ABTS radicals scavenging effect of PSC-x eutectogels were tested following the instructions of ABTS free radicals scavenging kit. The amount of eutectogel samples was fixed to 1 mg/ml in the working solution.

1.5 In vitro anti-bacterial properties of PSC eutectogels

Escherichia Coli (*E. coli*, ATCC 25922) and *Staphylococcus aureus* (*S. aureus*, ATCC 6538) were employed to test the anti-bacterial properties of PSC-x eutectogels. The as-prepared PSC-x eutectogels were exposed to UV light for sterilization in advance and the sterile samples were incubated with bacterial suspension (10^6 CFU/mL) at a concentration of 1 mg/mL at 37°C. At prescribed time point, the optical density at 630 nm (OD_{630}) of the suspension were recorded to monitor bacterial growth. To explore the minimum inhibitory concentration of PSC-5 eutectogel, the sterile samples were incubated with bacterial suspension (10^6 CFU/mL) at different concentrations at 37°C for 6 h. Then the suspension was diluted 10^5 times which were spread on agar plates and cultured at 37°C for 12 h. Finally, the colony-forming units (CUF) were counted. The antibacterial ratio of PSC-5 eutectogel was calculated to the following equation:

$$Antibacterial\ ratio\ (\%) = (1 - \frac{CFU_{sample}}{CFU_{control}}) \times 100\%$$

1.6 Transformation mechanism of PSC-5 eutectogel

The morphology of as-prepared and transformed PSC-5 eutectogel was observed using a scanning electron microscope (Apreo S HiVoc, Thermo Fisher) equipped with a cryo-SEM preparation system (PP3010T, Quorum). The Raman spectra of as-prepared and transformed PSC-5 eutectogel were recorded on a high-resolution Raman spectrometer (HR evolution, Horiba) with excitation wavelength at 532 nm. The FT-IR spectra of PSC-5 eutectogel undergoing transformation were recorded on a FT-IR spectrometer (Nicolet iS50, Thermo Fisher) using attenuated total reflectance (ATR) mode. These spectra were further used for two-dimensional correlation spectroscopy (2DCOS) analysis using 2DCS software (professional edition,

ver 1.4B). In the contour maps, red colour was defined as positive, and blue colour was defined as negatives. The responsive order of different groups can be judged by Noda's rule.

1.7 Computational simulation

The interactions between SBMA and CA was optimized by density functional theory (DFT). The hybrid functional B3LYP that combine the three-parameter hybrid exchange functional of Becke and the correlation functional of Lee, Yang, and Parr and 6-31+G** basis set were used for the DFT calculation.[2] To improve the description on the non-bond interactions between two monomers in a dimer, Grimme's D3BJ dispersion correction was also combined with the B3LYP functionals. All the calculations were performed with Gaussian 16 package[3]. The binding energies was estimated from the energy differences between the combination and two monomers.

The release behavior of CA from PSC-5 eutectogels under water environment was investigated by molecular dynamics (MD) simulation using software GROMACS 2024 under Genera Amber Forcefield (GAFF).[4] First, the PSC-5 eutectogel consisting of 200 SBMA, 600 CA, and 5 EDMA was obtained with *HTPolynet*.[5] The system first underwent 50 ns' equilibration in the NPT ensemble at 298K at 1 bar of atmospheric pressure, and then it was solvated in a water cube of 10 nm^3 and subject to another 50 ns' equilibration in NPT to simulate the release of CA in water. TIP3P water model was used.[6] The time step size was 2fs. V-rescale and berendsen were used to control the temperature and the pressure, respectively. VMD 1.9.3 was used for visualization.[7] The contact area, interaction energy, and hydrogen bonding during the release process were statistically analyzed using module of "gmx sasa," "gmx energy," and "gmx hbond."

1.8 Barrier properties of PSC-5 eutectogel

Barrier properties of PSC-5 eutectogel were evaluated by water contact angle (WCA) assay, protein adsorption assay, bacteria adhesion assay and simulated wound protection assay against *S. aureus* invasion. The WCA of as-prepared PSC-5 eutectogel was measured on a contact angle meter (DSA25, Kruss). Bovine serum albumin (BSA) and lysozyme (Ly) were selected as model proteins and were co-incubated with PSC-5 eutectogel at 37°C with constant shaking. At different time points, the protein concentration was tested using a BCA protein assay kit. Specifically, the concentration of PSC-5 eutectogel in protein solution was set as 1mg/mL and the transformed PSC-5 eutectogel was fabricated by immersing a freshly-prepared eutectogel in PBS at 1mg/mL for at least 48h. For bacterial adhesion assay, bacterial suspension (10^8 CUF/mL) were co-incubated with PSC-5 eutectogel at 37°C for 24 h. Transparent film dressing (1626w,

3M) was used as control group. Then the residual bacteria on the surface were stained by DMAO and observed by confocal laser scanning microscope (LSM 700, Zeiss). Besides, the residual bacteria on the surface were fixed using 2.5% glutaraldehyde solution and dehydrated by gradient ethanol solution for SEM (Apreo S HiVoc, Thermo Fisher) observation. For wound protection assay, a 6-mm diameter wound was created on a fresh porcine skin which were then put on an agar plate. Sterile PSC-5 eutectogel with 12 mm diameter was used to cover the wound and 20 μL *S. aureus* suspension (10^8 CFU/mL) was dropped on the surface of eutectogel. No protection was set as control group. After co-culture for 24 h, the bacteria beneath the wound were collected and dispersed in 1 mL PBS. This bacterial suspension was diluted 10^5 times and then spread on new agar plates. After 12-hour culture, the number of bacterial colonies was counted.

1.9 Cytocompatibility assay

Mouse fibroblasts cells (L929) and human umbilical vein endothelial cells (HUVECs) were selected to access the cytocompatibility of the PSC-5 eutectogel. The cells were cultured in complete medium (DMEM supplemented with 1% penicillin-streptomycin and 10% fetal bovine serum) at 37 °C with 5% CO_2. The leach solution of PSC-5 eutectogel was prepared by immersing 10 mg PSC-5 eutectogel into 10 mL of complete medium and shaking at 37 °C for 24 h. Firstly, the L929 cells and HUVECs were seeded into 48-well plate at a density of 7000/well and incubated at 37 °C for 24 h. Then the culture medium was replaced by PSC-5 leaching solution (62.5 μg/mL). After culturing for 1 and 3 days, the cell viability was tested using CCK-8. The absorbance value at 450 nm was measured on a microplate reader (SpectraMax ABS plus, Molecular Devices). At the same time, the live and dead cells were stained by calcein-AM/PI solution for 15 min and observed by fluorescence microscope (IX71, Olympus). In addition, the cytoskeleton and cell nucleus were stained by TRITC-phalloidin and DAPI respectively according to the manufactures' instruction and observed by fluorescence microscope (IX71, Olympus).

1.10 Intracellular ROS scavenging assay

Mouse fibroblasts cells (L929) and human umbilical vein endothelial cells (HUVECs) were seeded into 48-well plated at density of 7000/well and cultured at 37 °C for 12 h. Then the culture medium was replaced by fresh complete medium containing 100 μM H_2O_2 and co-cultured for 24 h to stimulate intracellular ROS generation. Subsequently, the cells were incubated with 62.5 μg/mL PSC-5 leaching solution for 24 h and then washed with PBS and stained by ROS detect probe (DCFH-A) for 30 min. After PBS washing, the

cells were observed by fluorescence microscope (IX71, Olympus). The fluorescence intensity was analysed using ImageJ software.

1.11 Anti-inflammation assay

RAW264.7 cells were employed to accesses the anti-inflammation ability of the PSC-5 eutectogel which were cultured in the same way of L929 cells and HUVECs. The RAW264.7 cells were seeded into a 6-well plate at a density of 200000/well and cultured at 37°C for 12 h. Then the culture medium was replaced by complete medium containing 1 μg/mL LPS and co-cultured for 24 h to obtain M1 phenotype of RAW264.7 cells. Subsequently, the cells were incubated with 62.5 μg/mL PSC-5 leaching solution for 24 h for further tests.

1.11.1 Flow cytometry assay.

At the end of co-culture with PSC-5 leaching solution, the cells were collected and transferred into centrifuge tubes. The cells were firstly co-incubated with PE-CD86 antibody at 4°C for 30 min in the dark which were subsequently washed by PBS, fixed in 4% paraformaldehyde for 15 min, and treated with membrane-breaking agent (1:10 dilution) for 30 min. After PBS washing, the cells were co-incubated with APC-CD206 antibody at 4°C for 30 min in the dark. After PBS washing, the cells were resuspended in 1 mL PBS and then detected on a flow cytometer (Attune NxT, Thermo Fisher). The results were analysed by FlowJo software.

1.11.2 Real-time reverse transcription quantitative polymerase chain reaction (RT-qPCR) assay.

The relative mRNA expression level of IL-6, TNF-α and IL-10 was measured via RT-qPCR assay. The total RNA of RAW267.4 cells were extracted by TRIzol reagent. qPCR was performed using Bio-rad CFX Connect instrument. The primers were presented in Table S5, Supplementary Information. The relative mRNA expression levels, which were calculated using $2^{-\Delta\Delta CT}$ method, were normalized by the control group.

1.12 Establishment and treatment of *S.aureus*-infected wound model in rats

All the animal experiments were approved by the Medical Ethics Committee of Sichuan University (Approval number KS20240242) and were performed in compliance with the guidelines of Sichuan University. After anaesthesia by the inhalation of mixed isopentane gas (1-3%) and depilation, two 10-mm round wounds were created on the back of a Sprague Dawley rat (female, 6-week-old) using a biopsy punch. A 20-mm circular silicon splint was put on the wound area and fixed using 3-0 sterile sutures for reducing

the influence of skin shrinkage. The infected wound model was established by incubating 100 μL *S. aureus* suspension (10^8 CFU/mL) on the wound site for 2 days. After successful establishment of the infected wound model, the rats were randomly divided into three groups treated by commercial transparent dressings (1626w, 3M), CA solution (0.3 mg/mL) and sterile PSC-5 eutectogels (10 mm in diameter and 1 mm in thickness). The latter two groups were fixed to the wound site using 3M dressings. The treatments were conducted every 2 days meanwhile the dressings were changed. Specifically, the applied volume of CA solution was 150 μL for each treatment session. The day of first treatment was assigned as day 0. The wound area was analysed using ImageJ software. The wound tissues were collected at day 6 and day 12 for further characterization.

1.12.1 Histological staining.

The collected wound tissues were stored in the tissue fixative at 4 °C. Tissue slices were prepared and then stained with hematoxylin and eosin (H&E) and Masson's trichrome to observe the skin appearance and analyze the collagen percentage. In addition, immunofluorescence staining of inflammatory factors (IL-6 and TNF-α) was performed on the tissue slices. All the samples were oberved using a slice scanning system (VS200, Olympus).

1.12.2 RT-qPCR assay.

The collected wound tissues were stored in the tissue RNA preservation solution at -80 °C. The relative mRNA expression level of IL-6, TNF-α and IL-10 was measured via RT-qPCR assay whose procedures were similar to that of cell study. The primers were presented in Table S6, Supplementary Information and the calculation method was similar to that in cell experiments.

1.12.3 In-vivo biosafety evaluation.

Major organs including hearts, livers, spleens, lungs and kidneys were harvested at day 12 and stored in the tissue fixative at 4 °C for H&E staining. Meanwhile, blood sample was collected for blood routine examination using an animal blood cell analyzer (BC-2800Vet, Mindary).

1.13 Statistical information

All the experiments were conducted at least 3 times. The data were shown as Mean ± SD. One-way analysis of variance (ANOVA) followed by Tukey's post hoc test was used for comparisons among multiple groups and the student's test was used to determine the differences between two groups using Graphpad Prism

(9.5). The significant differences were expressed as * < 0.05, ** < 0.01, *** <0.001, **** <0.0001 and ns means no significant difference.

2 Supplementary Figures

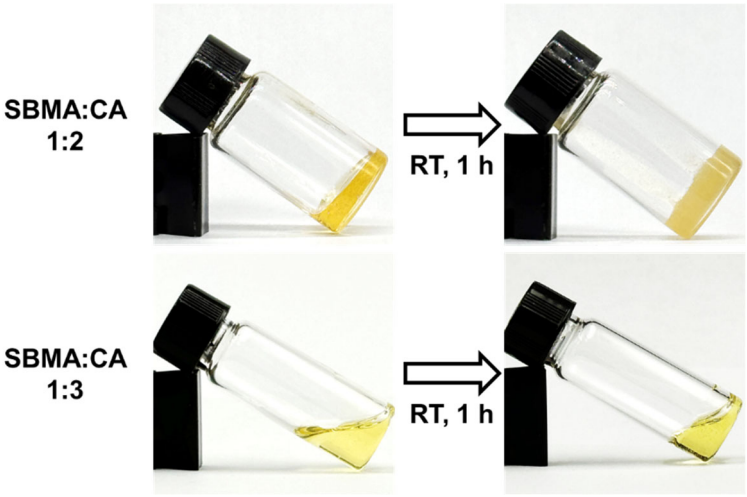

Fig. S1. Photographs of SC DES at different molar ratios.

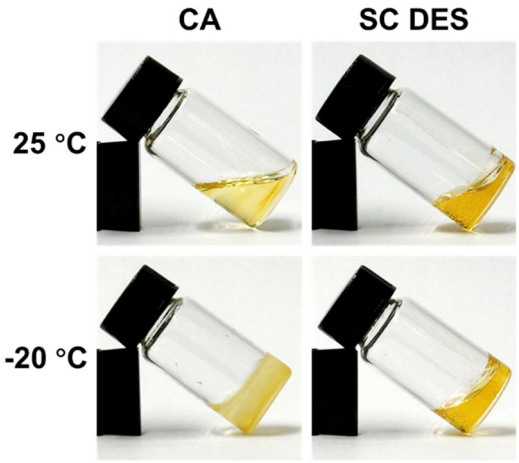

Fig. S2. Photographs of CA and SC DES at different temperature.

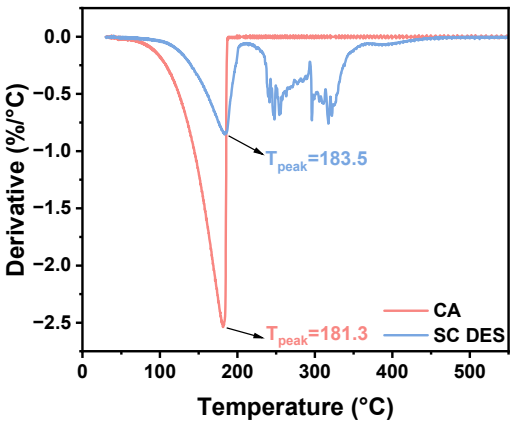

Fig. S3. Differential thermal gravimetric (DTG) analysis of CA and SC DES.

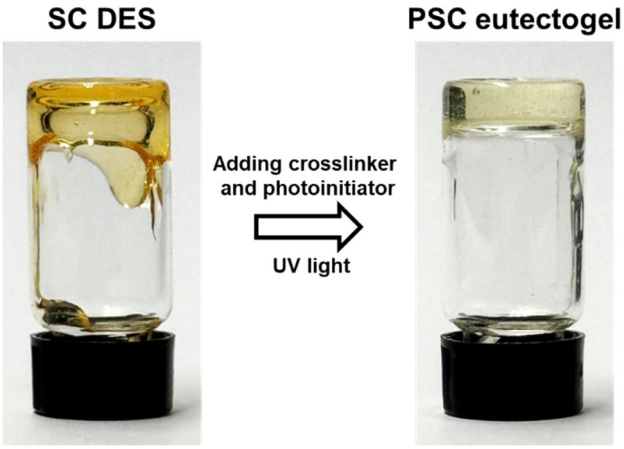

Fig. S4. Photographs of SC DES and PSC-5 eutectogel.

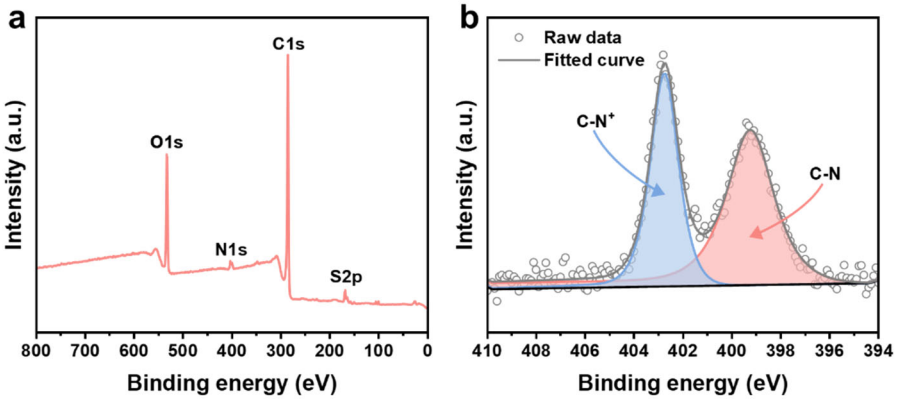

Fig. S5. (a) XPS spectrum and (b) high-resolution N 1s spectra of PSC-5 eutectogel.

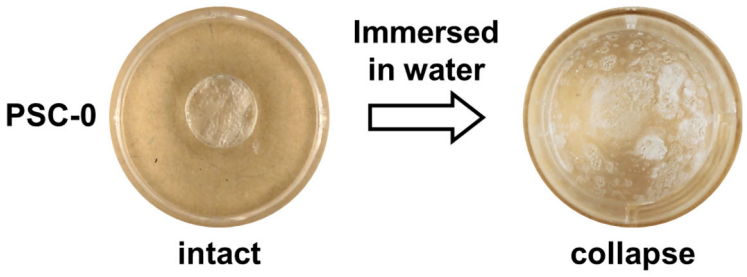

Fig. S6. Photographs of PSC-0 eutectogels before and after immerse in water.

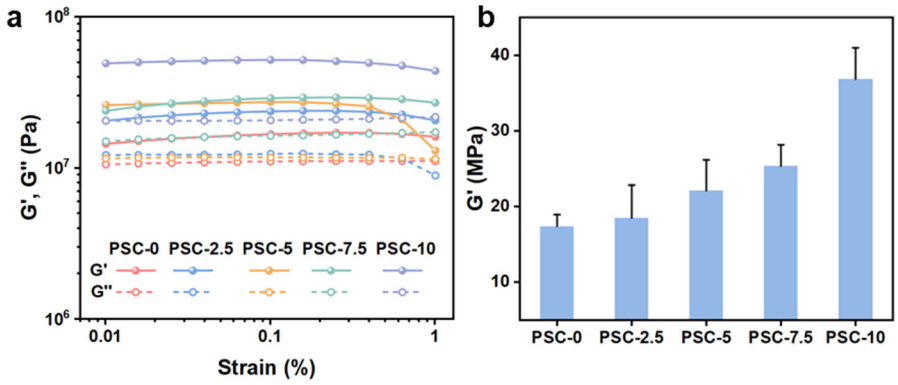

Fig. S7. (a) The G' and G'' of PSC eutectogels from strain amplitude sweep (0.01−1%) at a fixed angular frequency (25 Hz). (b) Average G' values of PSC eutectogels.

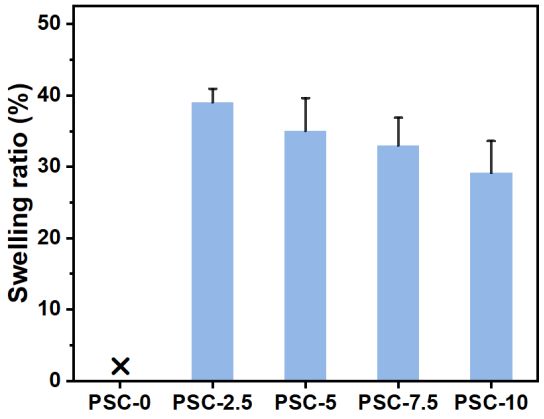

Fig. S8. Swelling ratios of PSC eutectogels.

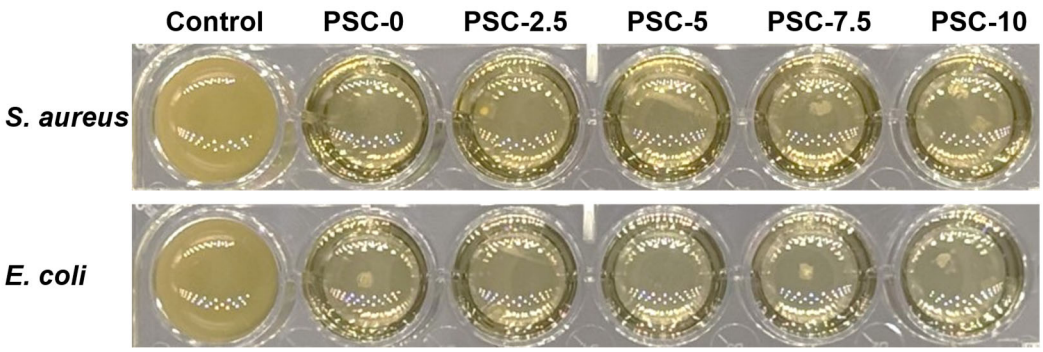

Fig. S9. Representative photographs of the bacteria after 24-hours coculture with PSC-x eutectogels.

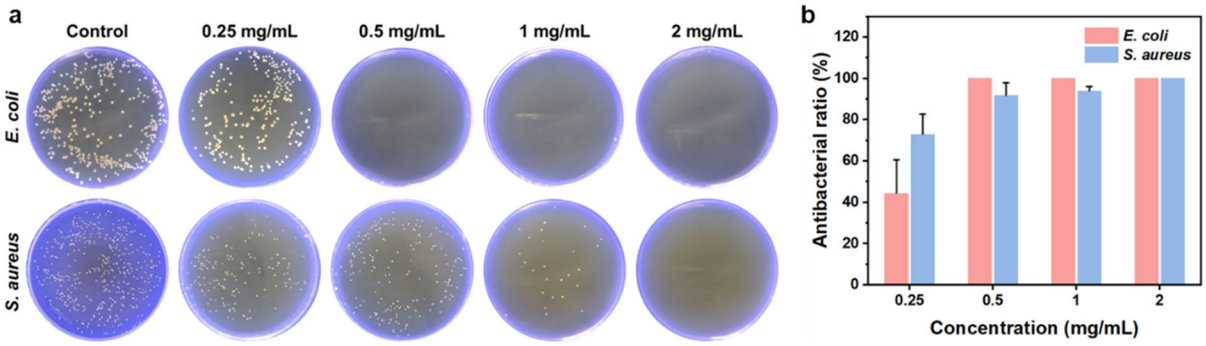

Fig. S10. (a) Representative photographs of survival bacteria after coculture with PSC-5 eutectogels for 6 h. (b) Antibacterial ratio of PSC-5 eutectogels at different concentrations.

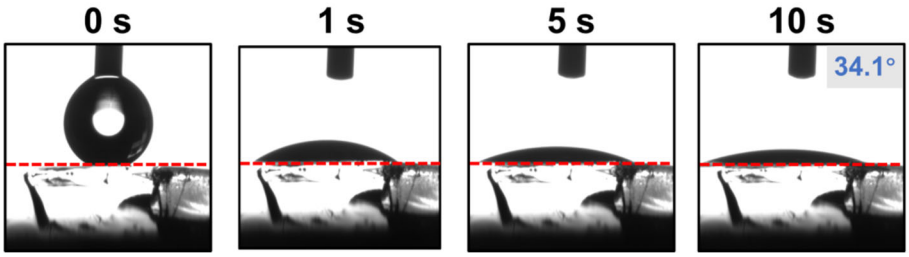

Fig. S11. Dynamic process of the changing water contact angles of PSC-5 eutectogels.

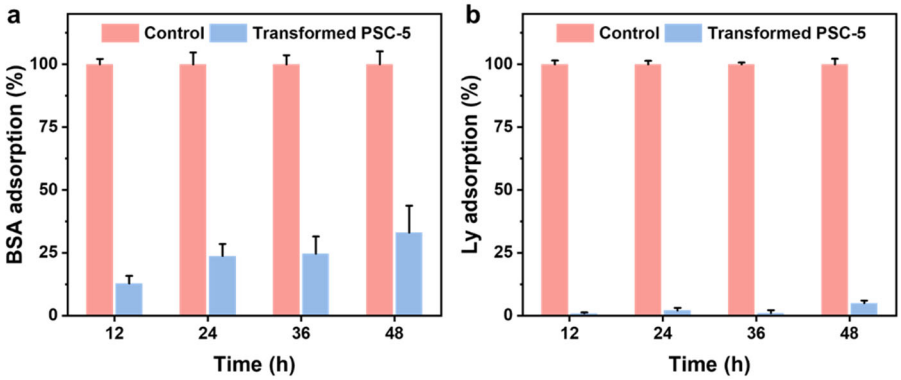

Fig. S12. Protein adsorption of the transformed PSC-5 eutectogel immersed in (a) BSA and (b) Ly solution.

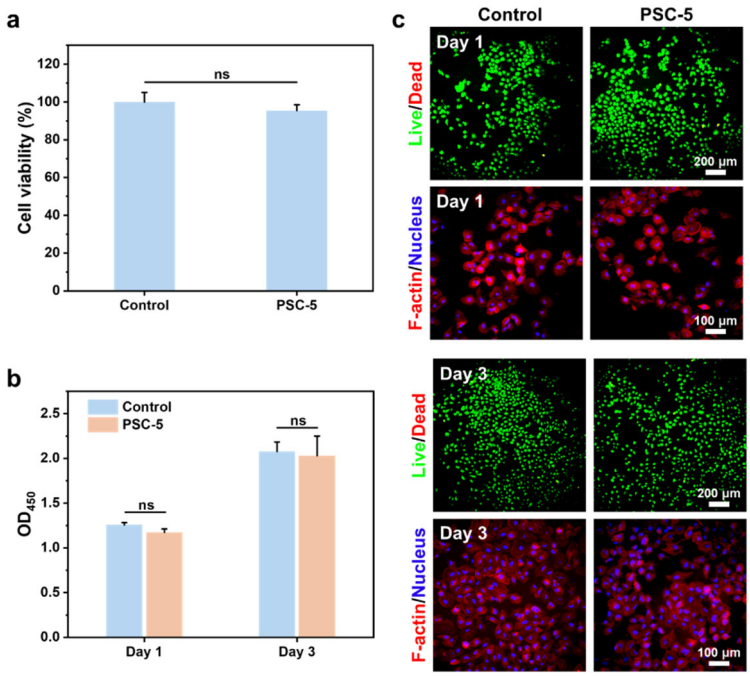

Fig. S13. (a) Cell viability of HUVEC after 24-hour coculture. (b) Optical density of HUVEC at day 1 and day 3. (c) Live/dead and cytoskeleton staining images of HUVEC at day 1 and day 3.

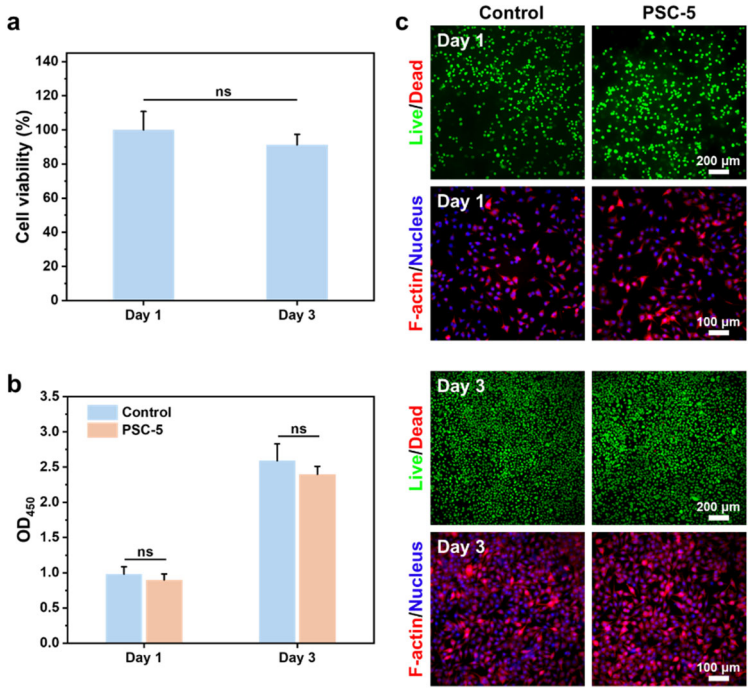

Fig. S14. (a) Cell viability of L929 cells after 24-hour coculture. (b) Optical density of L929 cells at day 1 and day 3. (c) Live/dead and cytoskeleton staining images of L929 cells at day 1 and day 3.

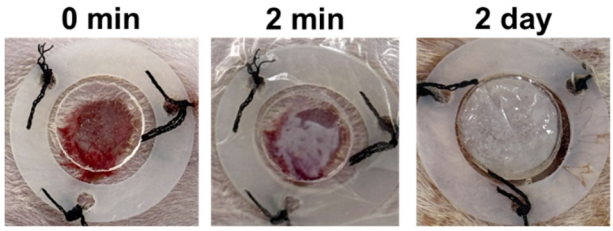

Fig. S15. Photographs of the network structure transformation of PSC-5 eutectogel during treatment of infected wound model.

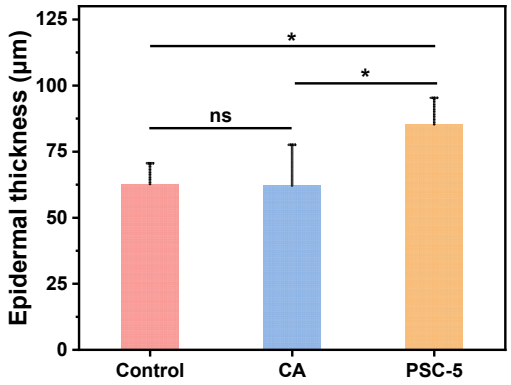

Fig. S16. Quantitation of the epidermal thickness from the H&E images at day 12.

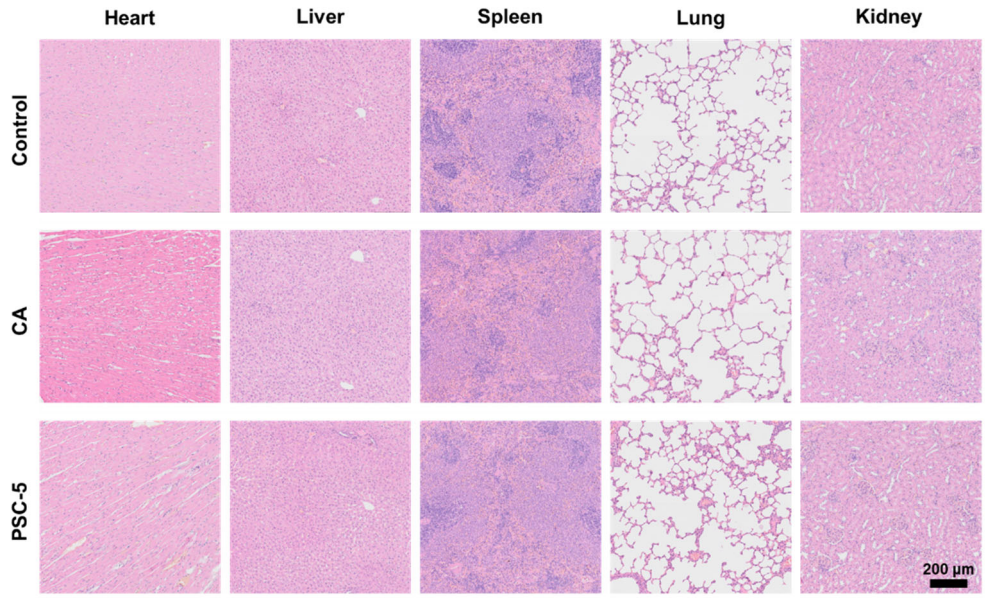

Fig. S17. Representative H&E images of the major organs of the rats with different treatment after 12 days.

3 Supplementary tables

Table S1. The kinetics of in-vitro CA release from PSC-2.5 and PSC-5 eutectogels.

Model	PSC-2.5 [b)]	PSC-5 [b)]
Zero order ($Q=k_1*t+a$)	$Q=6.23t+4.14$ $R^2=0.986$	$Q=3.65t+14.09$ $R^2=0.971$
First order ($Q=1-e^{-mt}$)	$Q=1-e^{-0.093t}$ $R^2=0.985$	$Q=1-e^{-0.073t}$ $R^2=0.987$
Ritger-peppas ($Q=k_2*t^n$) [a)]	$Q=8.72*t^{0.88}$ $R^2=0.992$	$Q=11.49*t^{0.65}$ $R^2=0.991$
Higuchi ($Q=k_3*t^{0.5}$)	$Q=17.2*t^{0.5}$ $R^2=0.828$	$Q=16.2*t^{0.5}$ $R^2=0.954$

[a)] n is characteristic exponent for distinguishing release mechanisms.

[b)] The data were fitted within Q<60%.

Table S2. The results of multiplication on the signs of each cross-peak in synchronous and asynchronous spectra.

	1043	1177	1200
1043		+	-
1177			+
1200			

Table S3. Biosafety parameters by blood routine examination.

	Normal range	Control	CA	PSC-5 eutectogel
WBC [a] (10^9 g/L)	2.9-15.3	15.63±4.01	12.13±1.96	13.30±6.21
LYMPH# [b] (10^9 g/L)	2.6-13.5	11.17±2.50	8.87±1.88	9.00±4.17
MON# [c] (10^9 g/L)	0.0-0.5	0.43±0.19	0.37±0.55	0.40±0.22
GRAN# [d] (10^9 g/L)	0.4-3.2	3.10±0.50	2.90±0.79	2.70±0.90
LYMPH% [e]	63.7-90.1	71.77±3.37	72.70±7.61	67.27±1.99
MON% [f]	1.5-4.5	3.07±0.17	2.93±0.34	3.47±0.46
GRAN% [g]	7.3-30.1	25.17±3.24	24.37±7.31	29.27±1.58
RBC [h] (10^{12} g/L)	5.60-7.89	6.16±0.19	6.29±0.28	6.37±0.18
HGB [i] (g/L)	120-150	144.00±4.97	141.67±5.44	148.67±8.38
HCT% [j]	36-46	33.10±0.94	32.53±1.33	34.03±1.30
MCV [k] (fL)	53.0-68.8	53.77±1.47	51.83±1.31	53.43±1.23
MCH [l] (pg)	16.0-23.1	23.33±0.88	22.50±0.45	23.30±0.88
MCHC [m] (g/L)	300-341	435.00±5.10	435.00±2.94	436.00±7.48
RDW% [n]	11.0-15.5	10.07±0.25	10.33±0.34	9.80±0.28
PLT [o] (10^9 /L)	100-1610	755.67±124.45	827.00±497.87	883.00±106.97
MPV [p] (fL)	3.8-6.2	5.83±0.29	5.70±0.50	5.47±0.05

[a] WBC, white blood cell count; [b] LYMPH#, lymphocyte count; [c] MON#, monocyte count; [d] GRAN#, granulocyte count; [e] LYMPH%, percentage of lymphocyte; [f] MON%, percentage of monocyte; [g] GRAN%, percentage of granulocyte; [h] RBC, red blood cell count; [i] HGB, hemoglobin; [j] HCT%, hematocrit; [k] MCV, mean corpusular volume; [l] MCH, mean corpusular hemoglobin; [m] MCHC, mean corpusular hemoglobin concerntration; [n] RDW, red blood cell volume distribution width; [o] PLT, plateletocrit; [p] MPV, mean platelet volume.

Table S4. Composition of PSC-x eutectogels.

	SBMA/mg	CA/mg	EDMA/mg	I1173/mg
PSC-0	279.35	450.66	0	3.28
PSC-2.5	279.35	450.66	4.96	3.37
PSC-5	279.35	450.66	9.92	3.45
PSC-7.5	279.35	450.66	14.87	3.53
PSC-10	279.35	450.66	19.82	3.61

Table S5. Primer sequences for RT-qPCR in cell experiments.

Target gene	Forward primer sequence	Reverse primer sequence
GAPDH	CCTCGTCCCGTAGACAAAATG	TGAGGTCAATGAAGGGGTCGT
IL-6	CCCCAATTTCCAATGCTCTCC	CGCACTAGGTTTGCCGAGTA
TNF-α	GTGCCTATGTCTCAGCCTCTTCTC	GTTTGTGAGTGTGAGGGTCTGG
IL-10	AATAAGCTCCAAGACCAAGGTGT	CATCATGTATGCTTCTATGCAGTTG

Table S6. Primer sequences for RT-qPCR in animal experiments.

Target gene	Forward primer sequence	Reverse primer sequence
GAPDH	CTGGAGAAACCTGCCAAGTATG	GGTGGAAGAATGGGAGTTGCT
IL-6	GAGTTGTGCAATGGCAATTCTG	ACGGAACTCCAGAAGACCAGAG
TNF-α	CCACCACGCTCTTCTGTCTACTG	TGGGCTACGGGCTTGTCACT
IL-10	ACAATAACTGCACCCACTTCCC	CCAAGTAACCCTTAAAGTCCTGC

4 Supplementary notes

Note S1. Correlations between rheological property and molecular chains mobility.

Rheological analysis has been widely utilized to study the mechanical property and the interaction between polymer and solvents for polymeric gels. A power correlation function was proposed to illustrate the frequency dependence of the dynamic rheological properties:

$$G'(\omega) \sim k\omega^n$$

Where the k depends on the flexibility of molecular chains and crosslinks and on the crosslinking density at gel point, and the n, critical relaxation component, corelates with the molecular mobility.

Note S2. Correlations between solid state NMR and molecular chains mobility.

The molecular mobility can be inferred from a simple free induction decay (FID) signal, which usually contains information about both rigid and mobile components. By combination of magic sandwich echo (MSE) FID and Hahn echo decay, a fully refocused FID of the eutectogels can be obtained. The decay of the rigid and flexible phase signals can be fitted with the corresponding functions to provide quantitative information about the components of the sample with different segmental mobilities. The FID shape was fitted to a linear combination of Gaussian function and two exponential functions:

$$A(t) = A_0(f_{rigid} \exp\left(-\frac{t}{T_{2,rigid}}\right)^2 + f_{inter} \exp\left(-\frac{t}{T_{2,inter}}\right)^2 + f_{mobile} \exp\left(-\frac{t}{T_{2,mobile}}\right)^2)$$

Where f_{rigid}, f_{inter}, and f_{mobile} were fractions for rigid, intermediate, and mobile components, and $T_{2,\,rigid}$, $T_{2,\,inter}$, and $T_{2,\,mobile}$ were the corresponding apparent relaxation times, respectively.

Reference

[1] J. Xiong, M. Duan, X. Zou, S. Gao, J. Guo, X. Wang, Q. Li, W. Li, X. Wang, F. Yan, *Journal of the American Chemical Society* **2024**, 146, 13903.

[2] P. J. Stephens, F. J. Devlin, C. F. Chabalowski, M. J. Frisch, *The Journal of Physical Chemistry* **1994**, 98, 11623.

[3] M. J. Frisch, G. W. Trucks, H. B. Schlegel, G. E. Scuseria, M. A. Robb, J. R. Cheeseman, G. Scalmani, V. Barone, G. A. Petersson, H. Nakatsuji, X. Li, M. Caricato, A. V. Marenich, J. Bloino, B. G. Janesko, R. Gomperts, B. Mennucci, H. P. Hratchian, J. V. Ortiz, A. F. Izmaylov, J. L. Sonnenberg, Williams, F. Ding, F. Lipparini, F. Egidi, J. Goings, B. Peng, A. Petrone, T. Henderson, D. Ranasinghe, V. G. Zakrzewski, J. Gao, N. Rega, G. Zheng, W. Liang, M. Hada, M. Ehara, K. Toyota, R. Fukuda, J. Hasegawa, M. Ishida, T. Nakajima, Y. Honda, O. Kitao, H. Nakai, T. Vreven, K. Throssell, J. A. Montgomery Jr., J. E. Peralta, F. Ogliaro, M. J. Bearpark, J. J. Heyd, E. N. Brothers, K. N. Kudin, V. N. Staroverov, T. A. Keith, R. Kobayashi, J. Normand, K. Raghavachari, A. P. Rendell, J. C. Burant, S. S. Iyengar, J. Tomasi, M. Cossi, J. M. Millam, M. Klene, C. Adamo, R. Cammi, J. W. Ochterski, R. L. Martin, K. Morokuma, O. Farkas, J. B. Foresman, D. J. Fox, Wallingford, CT 2016.

[4] a)V. Kumar, K. S. Rane, S. Wierzchowski, M. Shaik, J. R. Errington, *Industrial & Engineering Chemistry Research* **2014**, 53, 16072; b)J. Wang, R. M. Wolf, J. W. Caldwell, P. A. Kollman, D. A. Case, *Journal of Computational Chemistry* **2004**, 25, 1157.

[5] M. Huang, C. F. Abrams, *SoftwareX* **2023**, 21, 101303.

[6] a)W. L. Jorgensen, J. Chandrasekhar, J. D. Madura, R. W. Impey, M. L. Klein, *The Journal of Chemical Physics* **1983**, 79, 926; b)E. Neria, S. Fischer, M. Karplus, *The Journal of Chemical Physics* **1996**, 105, 1902.

[7] W. Humphrey, A. Dalke, K. Schulten, *Journal of Molecular Graphics* **1996**, 14, 33.